ISSN 1063-7826, Semiconductors, 2012, Vol. 46, No. 7, pp. 948–956. © Pleiades Publishing, Ltd., 2012.

PHYSICS OF SEMICONDUCTOR DEVICES

Influence of Irradiation with Neutrons on the Characteristics of the Voltage Terminating Structure in Silicon Radiation Detectors[1]

V. K. Eremin^, N. N. Fadeeva, E. M. Verbitskaya, and E. I. Terukov

Ioffe Physical–Technical Institute, Russian Academy of Sciences, St. Petersburg, 194021 Russia

^e-mail: Vladimir.Eremin@mail.ioffe.ru

Submitted December 26, 2011; accepted for publication December 30, 2011

Abstract—The distribution of potentials over a voltage terminating structure (VTS) has been studied in silicon nuclear-radiation detectors irradiated with neutrons in the range of doses from 1×10^{10} to 5×10^{15} n_{eq}/cm^2, where the VTS represents a system of floating ring p^+–n junctions. It is shown that variation in the profile of an electric field in the bulk of the detector as the radiation dose is increased is the determining factor in the distribution of potentials over the VTS. The mechanisms of VTS operation at irradiation doses lower than 5×10^{14} n_{eq}/cm^2 are established: the distribution of potentials between the rings is accomplished by a punch-through mechanism in the inter-ring gap, while, at higher doses, the distribution is controlled by a current-related mechanism, which is based on the density of the electron—hole generation current flowing in the bulk of the detector. The suggested mechanisms of VTS operation are confirmed experimentally and by simulation.

DOI: 10.1134/S1063782612070081

1. INTRODUCTION

One of the stimuli to intense development of silicon nuclear-radiation detectors in the last decade was related to new problems in experimental high-energy physics. For example, study of the fundamental processes occurring in the early stages of development of the Universe, simulation of the ultimately condensed state of matter in neutron stars, the search for the Higgs boson, and a number of other global projects is only possible if special silicon detectors are used. The largest, already established installations, such as the Large Hadron Collider (LHC) at CERN (Switzerland), and TEVATRON at the Fermi laboratory (USA), use hundreds of square meters of silicon stripped and pixel detectors, which exceeds by several times the previous year's production of semiconductor detectors wordwide. These problems required the development of new technologies and structures for detectors; it was also required to perform a large number of studies of the properties of high-resistivity silicon under conditions of irradiation with high-intensity fluxes of relativistic particles.

Successful operation of the largest experimental installations CMS and ATLAS at CERN with a large number of silicon detectors stimulated the development of this line in experimental physics, which requires the provision of operation ability for the silicon part of the installation at doses exceeding the attained limit of 2×10^{14} n_{eq}/cm^2 by tenfold. One of the aspects in solving this problem is a study of the effect of high doses of relativistic particles on elements of the detector's structure, which provide its stable current–voltage (I–V) characteristics.

As is known, irradiation of silicon with high-energy particles brings about the formation of radiation defects, including those that have energy levels in the band gap and, thus, are electrically active. Related to this is the process of capture of nonequilibrium charge carriers which gives rise to a decrease in the amplitude of the signal formed by a detected particle and modifies the distribution of the electric-field strength in the sensitive area of the detector, bringing about, for example, a loss in the position sensitivity of the detector. The processes of the generation of charge carriers via radiation levels at the midgap bring about an increase in the dark current of the detector and a decrease in its signal-to-noise ratio.

In thus study, we investigated the effect of irradiation with neutrons at doses as high as 5×10^{15} n_{eq}/cm^2 on the properties of ring structures, which surround the sensitive area of the detector and are designed to provide a gradual decrease in the potential from the central sensitive area to the detector's periphery (in what follows, we use the abbreviation VTS, which stands for voltage terminating structure [1]). This makes it possible to prevent the formation of regions with a high electric field at the radiation-sensitive contact and the flow of surface and peripheral currents, thus attaining stabilization of the device's operation. Such structures consist of a series of concentric (closed or opened) rings, which constitute floating (not connected to any fixed potential) p–n junctions,

[1] The article is published in the original.

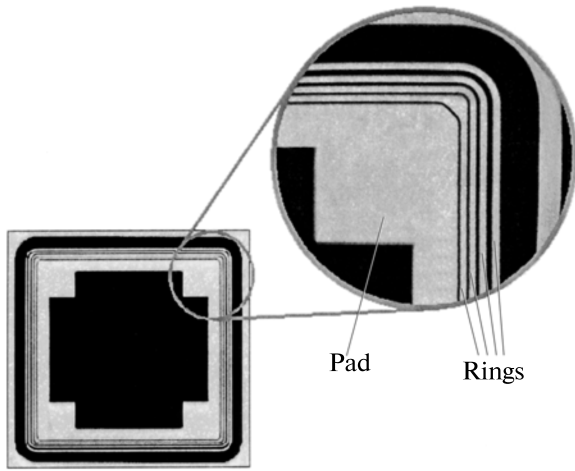

Fig. 1. A photograph of the detector under study.

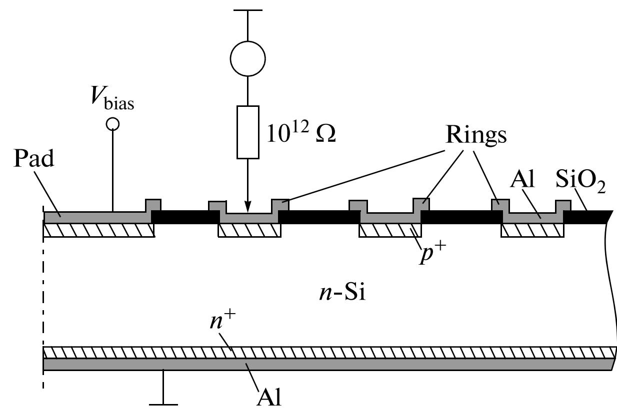

Fig. 2. Schematic representation of a fragment of the detector structure illustrating the basics of measurements of the distribution of the potentials over the VTS.

the number and technology of which is optimized for a specific type of device and conditions of its operation.

We concentrate are attention on the effect of irradiation on the main VTS characteristic, i.e., the distribution of potentials over rings in the structure. Measurements were performed for the samples fabricated in the context of a project for the development of proton detectors for the TOTEM experiment at CERN. The studies are included in a program of efforts aimed at the development of detectors for modernization of the experiments at the LHC, and also are important for the development of installations involving silicon detectors in the context of the FAIR program at GSI (Germany).

2. SAMPLES FOR STUDIES

We studied the samples of silicon detector structures based on p^+–n junctions surrounded by a system of floating p^+ rings. A photograph of the detector is shown in Fig. 1. The samples were fabricated from dislocation-free float-zone silicon produced by TOPSIL Co. (USA); the Si resistivity was 7 kΩ cm. All structures featured the same topology with the area of the central radiation-sensitive (the so-called pad electrode, or just pad) p^+ contact equal to 5×5 mm^2. The VTS consisted of four closed floating p^+ rings separated by inter-ring spacings; the surface of the rings was passivated with a SiO_2 layer. The rear ohmic contact was formed in the shape of a continuous heavily doped n^+-type layer. The thickness of the structures was 300 μm. Detectors were irradiated with 1-MeV neutrons in the range of doses from 1×10^{10} to 5×10^{15} n_{eq}/cm^2, which, in fact, span the expected range of radiation effects on internal track detectors in the main experiments in the LHC after tenfold increase in the beam intensity.

Measurements of the potentials' distribution over the VTS of the detectors were performed using an installation with microprobes and a Keithley-487 picoampere meter equipped with a built-in power source (Fig. 2). The probe of this device was sensitive to the potential and had the resistance 10^{12} Ω, which ensured the conditions of floating potential for a ring during the course of potential measurements on this ring; the central p^+–n junction was biased in the reverse direction with the voltage V_{bias} with the rear n^+ contact grounded.

3. EXPERIMENTAL RESULTS

Figure 3 shows the dependences of the potentials φ at the rings on the reverse voltage V_{bias} for detectors irradiated with neutrons in the range of doses from 1×10^{10} to 5×10^{15} n_{eq}/cm^2. The plots show the magnitudes of the negative voltage at the central electrode of the samples and potentials at the VTS' rings. The solid curve shows a variation in the potential of the central p^+ contact $\varphi_{pad} = V_{bias}$; curves *1*–*4* represent potentials from the first to fourth rings, respectively.

For a sample irradiated with a low dose 1×10^{10} n_{eq}/cm^2 (Fig. 3a), the distribution of the potential over the VTS rings features a characteristic shape: as the voltage at the central contact is increased, there occurs a successive inclusion of floating rings at certain values of the voltage V_{bias} equal to the critical one V_{cr} with a subsequent increase in their potentials. It is worth noting that the voltage drop between the central electrode of the structure and the first ring V_{bias}–φ_1 features a slight stable increase but its value does not exceed 80 V, which ensures a stable I–V characteristic in a wide range of voltages (Fig. 4). The potential of the last ring also increases and, at V_{bias} = 400 V, attains 150 V, which is twice as large as the voltage drop between the remaining rings. It is evident that a further

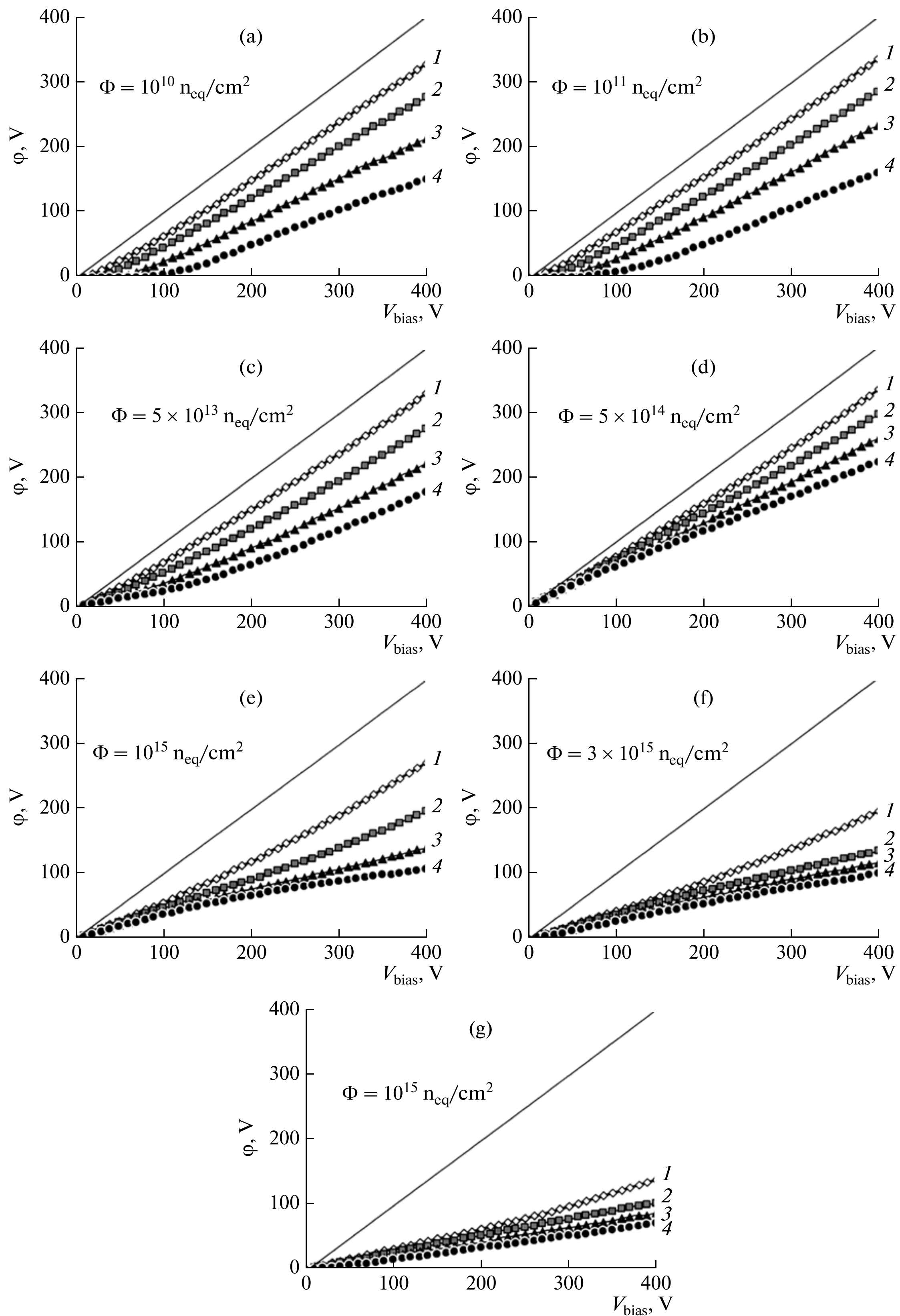

Fig. 3. Dependences of the potentials at the rings φ on the voltage V_{bias} applied to the central electrode for the samples irradiated with neutrons. The dose of irradiation was (a) 10^{10}, (b) 10^{11}, (c) 5×10^{13}, (d) 5×10^{14}, (e) 10^{15}, (f) 3×10^{15}, and (g) 5×10^{15} n_{eq}/cm^2. The numbers of the curves correspond to the numbers of the rings starting with the internal ring. The solid line shows the potential of the central electrode.

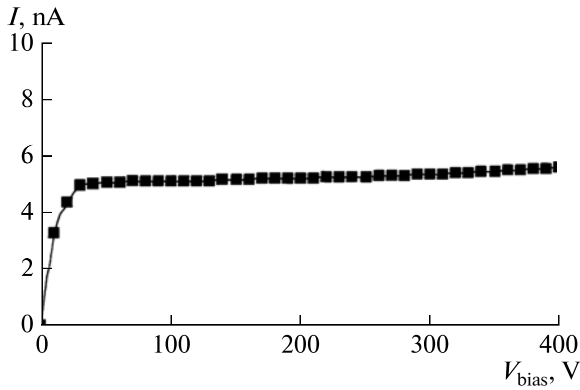

Fig. 4. *I–V* characteristics of the detector irradiated with a dose of 10^{10} n_{eq}/cm^2. Measurements were performed at the grounded inner ring.

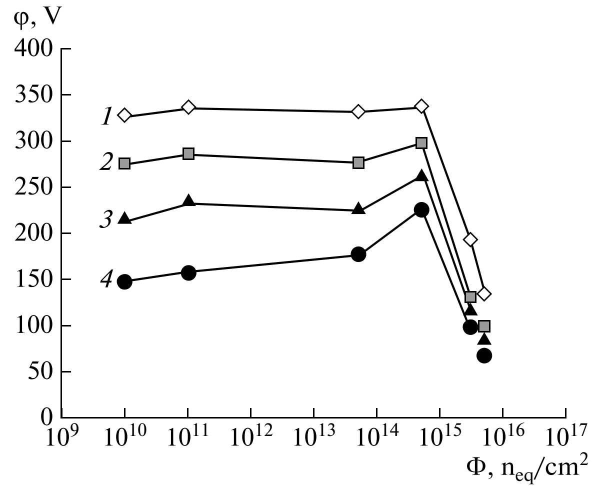

Fig. 5. Dependences of the distribution of the potentials over the detector's rings on the irradiation dose Φ at the reverse voltage V_{bias} = 400 V. The numbers of the curves correspond to the numbers of rings starting with the inner ring.

increase in the bias voltage applied to the diode can give rise to a breakdown of the peripheral ring itself (since the field is focused at its outer boundary) and to a successive avalanche-like process of breakdown of the remaining rings. Taking into account the above comment, we restricted the bias-voltage range to the value 400 V.

As the irradiation dose is increased, the value of the critical voltage V_{cr} for all rings decreases and becomes equal to zero at a dose of 5×10^{13} n_{eq}/cm^2 (Fig. 3c). For detectors irradiated with the dose 5×10^{14} n_{eq}/cm^2 (see Fig. 3d), the potentials at all rings increased in the entire range of applied voltages V_{bias} in comparison with the potential of the rings in detectors irradiated with lower doses.

In the initial portion of the voltage V_{bias} (0–200 V), the potentials at the rings are close to each other and effective division of the potentials is lacking. As the irradiation dose is further increased (Figs. 3e, 3g), the potentials at all rings become the same in the entire range of measured voltages, while the voltage drop between the central electrode and the first ring considerably increases.

In Fig. 5, we present the distribution of the potentials over the VTS for detectors irradiated with neutrons in the range of doses from 1×10^{10} to 5×10^{15} n_{eq}/cm^2 at the reverse voltage V_{bias} = 400 V. It can be seen from the plot that, as the dose is increased to 5×10^{14} cm^{-2}, the potentials of the rings increase, while the voltage drops between the rings. At a further increase in the dose, the potentials drastically decrease and effective division of the potentials over the VTS is lacking.

As was shown in studies of the mechanisms of the distribution of potentials over the detector's VTS before irradiation, the value of the electric field in the region of the inter-ring gap is the most important factor, which determines the difference in potentials between neighboring rings [1]. Irradiation of silicon diode structures brings about the generation of radiation defects with energy levels that affect the effective concentration N_{eff} in the space-charge region (SCR) and the corresponding profile of the electric field. In the case of irradiation of *n*-Si, compensation with acceptor levels mainly occurs; therefore, at low doses, the effective concentration N_{eff} in the detector's SCR decreases. In what follows, the sign of the space charge is changed from positive to negative, i.e., inversion of the space charge's sign takes place. The dependence of the effective concentration N_{eff} on the dose of irradiation with neutrons Φ can be calculated using the following parametric equation [2]:

$$N_{eff}(\Phi) = N_{d0}\exp(-\gamma\Phi) - \beta\Phi; \quad (1)$$

here, N_{d0} is the effective concentration before irradiation with $N_{d0} = N_{eff}(\Phi = 0)$; $\gamma = 8.8 \times 10^{-14}$ cm^2 is the coefficient of donor removal; and $\beta = 0.022$ cm^{-3} is the coefficient of acceptor introduction. According to Eq. (1), inversion occurs at the irradiation dose $\Phi = 1 \times 10^{13}$ n_{eq}/cm^2 for the silicon with the resistivity 7 kΩ cm ($N_{d0} = 6 \times 10^{11}$ cm^{-3}) used by us. As the dose of irradiation is further increased, the magnitude of N_{eff} increases.

In order to study the distribution of the electric field in the samples irradiated with various doses, we used the transient-current technique (TCT), which involves measurement of the shape of the structure's current response to the pulsed generation of nonequilibrium charge carriers in the sample [3, 4]. Figure 6 shows current pulses of the sensitive p^+–n junction under pulsed generation of nonequilbrium charge carriers in a layer with a thickness of about 10 μm, which was accomplished by illumination of the sensitive con-

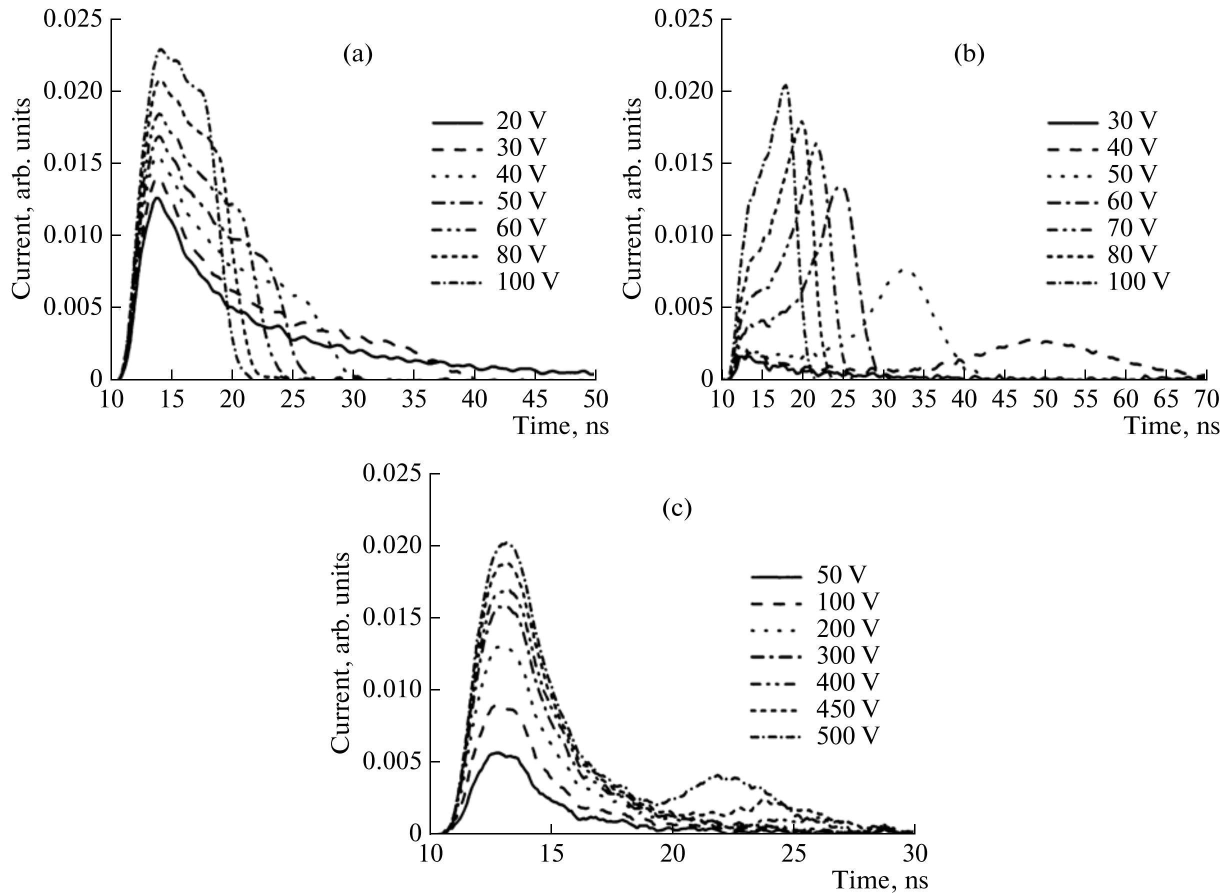

Fig. 6. Pulses of the transient current for sensitivity of the p^+–n junction of detectors under the incidence of laser pulses on the p^+ side. The irradiation doses were (a) 10^{11}, (b) 5×10^{13}, and (c) 10^{15} n_{eq}/cm^2.

tact's surface by a laser pulse with a duration of 0.7 ns (the wavelength is 670 nm). The instantaneous value for the arising transient current $i(t)$ is proportional to the drift velocity of a packet of charge carriers $v_{dr}(t)$; this packet moves in the region of an electric field of a completely depleted detector with the thickness d [4]; the transient current is written as

$$i(t) = \frac{1}{d} q v_{dr}(t) = \frac{1}{d} q \mu E(x, t), \quad (2)$$

where q is the elementary charge, d is the structure thickness, v_{dr} is the drift velocity of transported charge, μ is the mobility of charge carriers, and $E(x, t)$ is the profile of the electric field.

The shapes of the transient-current pulses shown in Figs. 6a–6c correspond to the incidence of the light pulses on the p^+-type side of the structure; in this case, a packet of electrons is transported in the bulk of the sample in the direction of the n^+-type contact. Since the instantaneous value of the current is proportional to the drift velocity, which is an increasing function of an electric field, the slope of the pulse top uniquely determines the field gradient and, consequently, the sign of the bulk charge. We may then conclude that, in the p^+–n structure subjected to irradiation with a low dose 1×10^{11} n_{eq}/cm^2 (Fig. 6a), the space charge remains positive (the maximum of the field is located near the p^+-type contact). At a dose of 5×10^{13} n_{eq}/cm^2, the amplitude of the pulses increases with time (Fig. 6b). Consequently, the space charge becomes negative and the maximum of the electric-field strength shifts to the n^+ contact, while the ring structure is found to be in the low-field region. At larger doses (1×10^{15} n_{eq}/cm^2), the electric field near the n^+ contact is dominant; however, a decrease in the value of the transported charge q caused by the capture of charge carriers at deep levels brings about a decrease in the pulse amplitude with time (Fig. 6c). A drastic decrease in current at pulse completion is attained only at $V = 400$ V, which indicates that there is no total depletion of the structure at lower voltages.

4. DISCUSSION

As was shown previously [1], the distribution of the potentials over the VTS of unirradiated detectors is

described in terms of an injection model of current flow through the inter-ring gaps in the VTS. In the case where the sensitive $p^+–n$ junction is reverse biased, the ring potential remains equal to zero until a high critical voltage $V_{bias} = V_{cr}$. At this voltage, the so-called punch-through of the gap occurs, i.e, injection of holes from the p^+-type region of the ring into the inter-ring gap begins and the ring potential becomes different from zero. A further increase in the applied voltage brings about an increase in the ring potential. The conditions required for a punch-through of the inter-ring gap depend on the distribution of the electric-field strength in the gap and is determined by the competition between the normal and tangential (parallel to the surface of the gap) vectors of the electric field. Injection is stimulated by the tangential component of the electric field, whereas the normal component inhibits injection by directing the charge carriers to the diode bulk, thus interrupting the inter-ring current. An increase in the normal component is responsible for an increase in the voltage drop between rings as the voltage at the $p^+–n$ junction is increased.

It follows from the plots shown in Figs. 3a and 3b that the distribution of the potentials over the VTS for detectors irradiated with low doses of neutrons (1×10^{10} and 1×10^{11} n_{eq}/cm^2) is consistent with the injection model of current flow through the inter-ring gaps in the VTS. An increase in the ring potentials starts with a certain value of the critical voltage V_{cr} and continues as the applied voltage V_{bias} is increased.

As the irradiation dose is increased in the range $10^{10}–10^{11}$ n_{eq}/cm^2, the absolute value of the effective concentration of the bulk charge decreases according to Eq. (1), which, correspondingly, reduces the inhomogeneity of the electric field and, respectively, the field strength at the p^+ contacts. This systematic feature brings about a decrease in V_{cr} and a slight decrease in the difference between the potentials in the rings as the dose is increased. At these doses, the highest electric-field strength is located at the p^+ contact and, thus, a nonzero normal to the surface field exists at any voltage in the structure (including for the case of contact potential difference). Due to this, an increase in the potentials at the rings starts at $V_{cr} > 0$. With irradiation, the highest value of the electric-field strength decreases, which facilitates attainment of the punch-through condition between the rings and manifests itself in a decrease in V_{cr}.

The operation of the VTS radically changes at a dose of 5×10^{13} n_{eq}/cm^2 (Fig. 3c): V_{cr} becomes equal to zero for all rings, while the dependences of the ring potentials on V_{bias} are significantly linearized. These changes are in qualitative agreement with the results of studying the electric-field distribution in the detector, which are illustrated by the pulses in Fig. 6b. At a dose of 5×10^{13} n_{eq}/cm^2, the highest electric field is located near the n^+ contact; at a voltage lower than the depletion voltage for the structure, the rings on the p^+ side are found to be in the zero field. It is evident that, under these conditions, the punch-through mechanism for inter-ring gaps in the VTS cannot be operative in the electric field of the/a reverse-biased $p^+–n$ junction. Indeed, in a partially depleted structure, the conducting base near the p^+-type contact connects, in fact, all the VTS' rings to each other; the leakage current of the $n^+–n$ junction, which is in contact with the n^+-type side of the chip, flows over the end plane of the chip and then through the VTS, thus increasing the potential of the peripheral fourth ring and the entire VTS as a whole. Therefore, in the case of depletion of the structure (depletion is attained at 75 V), a drop in the potential arises between rings according to the standard punch-through mechanism, however, now at a level of nonzero potential of the peripheral ring.

At a dose of 5×10^{14} n_{eq}/cm^2, an increase in the potentials of all VTS rings is observed; as a result, the drop in the voltage at the periphery of the detector reaches a value of more than 50% of the voltage V_{bias} applied to the structure. It is noteworthy that, in this case, the potentials of the rings increase virtually linearly in the entire range of voltages; an appreciable difference between the potentials of neighboring rings arises at a reverse voltage V_{bias} higher than 200 V (Fig. 3d). This value is found to be several times smaller than the depletion voltage, which, according to [5], is equal to about 750 V. This fact is direct evidence of the existence of two maximums for the electric field in heavily irradiated $p^+–n–n^+$ structures; these maximums are located near opposite contacts [6]. The main depleted region, on which drops the large portion of the applied voltage, is situated near the n^+-type contact. An additional region of the electric field at the p^+-type contact is formed due to the capture of holes thermally generated in the bulk of the structure and is the cause of the appearance of a potential difference between rings. It is evident that a difference in the potential of rings is found to be insignificant since the potential drop across the field layer near the p^+-type contact is severalfold smaller than in the main depleted region.

At higher doses, $1 \times 10^{15}–5 \times 10^{15}$ n_{eq}/cm^2, the tendency in the variation in potentials becomes reverse (Figs. 3e–3g). As the dose is increased, the potentials of the VTS' rings decrease and an effective division of the potentials is in fact lacking (Fig. 5). For example, at a dose of 5×10^{15} n_{eq}/cm^2, 80% of the potential drops between the central electrode and the first VTS ring. The cause of such a large difference between the potential of the central contact in the structure and that of the neighboring floating ring may be the dominance of the current-related mechanism of electric-field formation in the bulk of the structure. The dark current in the structure increases in proportion to the irradiation dose and, at doses $\sim 10^{15}$ n_{eq}/cm^2, reaches

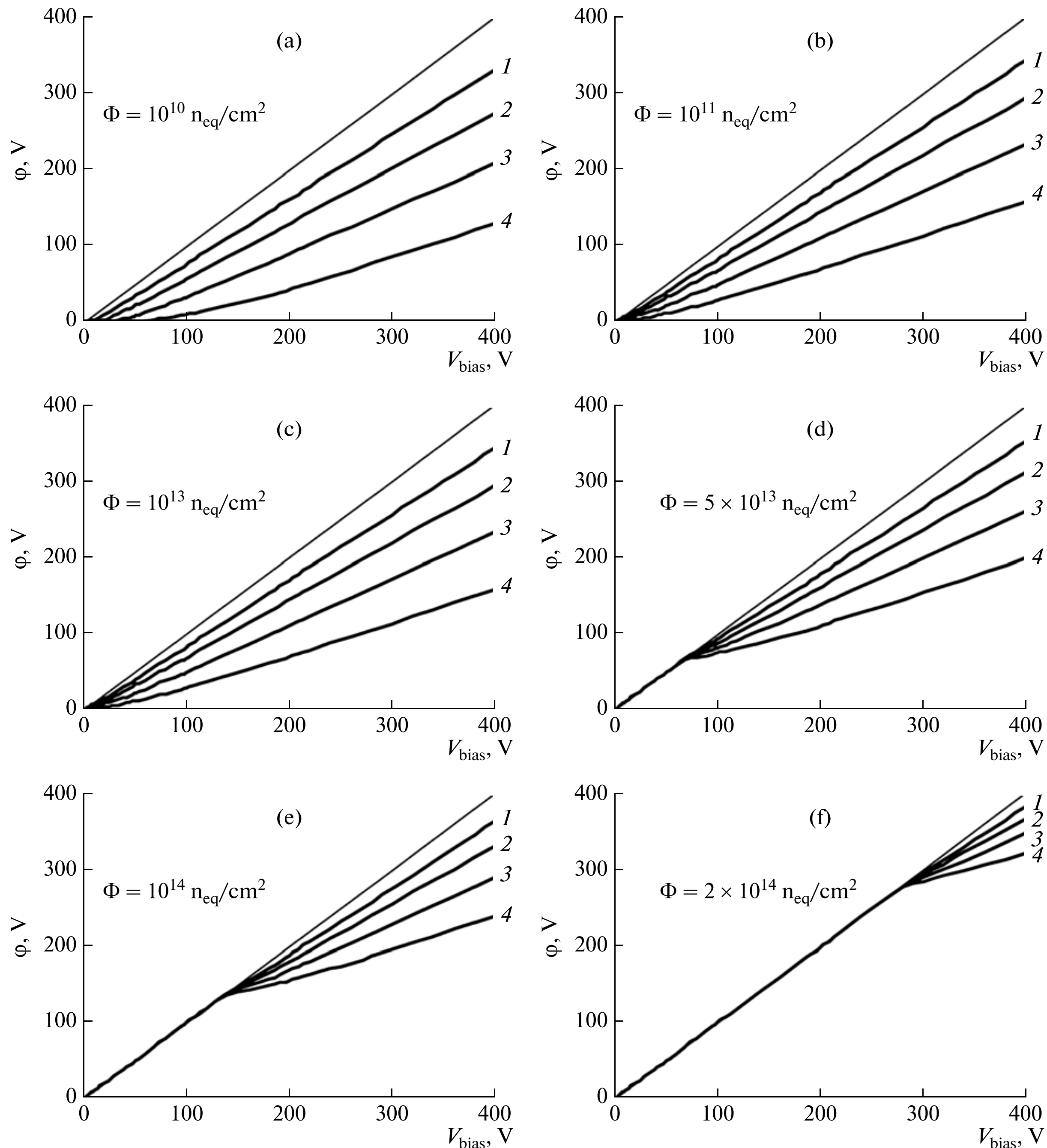

Fig. 7. Simulated dependences of the potentials at the rings φ on the voltage V_{bias} applied to the central electrode of the detectors. The irradiation dose was (a) 10^{10}, (b) 10^{11}, (c) 10^{13}, (d) 5×10^{13}, (e) 10^{14}, and (f) 2×10^{14} n_{eq}/cm^2. The numbers of the curves correspond to the numbers of the rings. The upper line represents the potential of the central electrode.

as high as tens of μA/cm^2/300 μm. At a high rate of current generation in the bulk and a significant concentration of radiation defects, which are capture centers for free charge carriers, an electric field is formed by the trapped charge of electrons and holes, i.e., this field mainly exists in regions where the current flows. On the p^+-type side, these include the region adjacent to the sensitive p^+–n junction where the main current of the structure is collected. The VTS' floating rings surrounding this region and isolating it from the central contact do not collect current and are situated away from the trajectories of holes drifting toward the p^+-type contact. As a consequence, a ring system is found in the region, in which the electric field is low and the potential is close to that of the rear n^+-type contact. This is completely consistent with the condi-

tions of the performed experiment since, at the highest dose of irradiation (5×10^{15} n_{eq}/cm^2), the thickness of the space-charge layer on the n^+-side does not exceed 100 μm at $V_{bias} = 400$ V. Therefore, the electric-field configuration is determined by the configuration of the lines of electrical-current flow in the base; this current forms the space charge by the mechanism of charge-carrier capture. Qualitatively, the interrelation between the electric-field distribution and the flowing current is given by the following expression:

$$\operatorname{div} E \propto qN_{tr} \propto f(\tau)(j_h - j_n); \quad (3)$$

here, q is the elementary charge; N_{tr} is the difference between the concentrations of captured electrons and holes; $f(\tau)$ is a function describing the probability of the capture of electrons and holes; and j_h and j_n are the electron and hole current densities, respectively. Since the hole current is dominant at the p^+-type contact, the value of $\operatorname{div} E$ is always positive; consequently, the maximum field is bound to be located at the surface of the p^+-type contact, which collects holes. The electric-field strength near the isolated rings is bound to be at a minimum and, as experiments show, there potential is close to that of the n^+-type contact.

5. SIMULATION OF THE DISTRIBUTION OF THE POTENTIALS OVER THE VTS

In order to explain the effect of capture of charge carriers of the dark current on the distribution of potentials over the VTS, we performed a computer simulation. Using the software package SILVACO-TCAD, we simulated a simplified structure of the detector, which is presented in Fig. 1. In the simulation, we disregarded the introduction of deep levels as a result of irradiation and, as a result, we disregarded the formation of the electric-field profile with two maximums near the p^+- and n^+-type contacts in the case of irradiation with high doses. The adjustable parameter was the effective impurity concentration, which was calculated as a function of the dose of irradiation using formula (1). For detectors irradiated with doses of no higher than 10^{13} n_{eq}/cm^2, i.e., prior to inversion of the space-charge sign, the detector model corresponded to the p^+–n–n^+ structure. At irradiation doses of higher than 10^{13} n_{eq}/cm^2, the model took into account the inversion of the space-charge sign and corresponded to a p^+–n–n^+ structure. The charge at the Si–SiO_2 interface was fixed and amounted to 3×10^{10} cm^{-3}.

Figure 7 shows the dependences of the potentials φ at the rings on the reverse voltage V_{bias} for detectors irradiated with neutrons in the range of doses from 1×10^{10} to 2×10^{14} n_{eq}/cm^2; the dependences were obtained as a result of experiments.

Comparison of the simulation results and experimental data shows that, at low doses of irradiation (up to 1×10^{13} n_{eq}/cm^2), the dependences of the distribution of the potentials over the VTS are similar; the above-described tendency towards a decrease in V_{cr} with an increase in the irradiation dose is observed. As the dose of irradiation is further increased beyond the inversion point, we may notice significant divergences. Simulation shows that the potentials of the rings and of the main junction are equal to each other as long as the depletion voltage of the detectors is not exceeded (for example, for a detector irradiated with a dose of 10^{14} n_{eq}/cm^2, the depletion voltage amounts to 150 V): all rings feature the same potential since they are found to be shorted by the conducting undepleted base region. In the range of voltages V_{bias} exceeding the voltage of complete depletion, the potential at the rings becomes different because the rings are found in the region of the electric field and the mechanism of the potentials' formation with the punch-through of inter-ring gaps becomes operative. These divergences result from the fact that the simulation disregarded the introduction of defects with deep levels, as a result of which the base acquires high resistivity, the process of the capture of charge carriers from the dark current becomes operative, and, as a consequence, a fundamentally different character of the electric-field distribution is observed.

6. CONCLUSIONS

The performed studies show that the radiation-induced degradation of a detector's bulk brings about disruption in the operation of the systems for stabilization of the characteristics of the p–n junction in addition to a reduction in the signal from detected particles. The determining mechanism in the case of an increase in the irradiation dose involves variation in the electric-field distribution in the detector's bulk and the replacement of the electrostatic mechanism for field formation in the SCR by a mixed mechanism with dominant influence of the density of the electron—hole generation current, which flows in the bulk. In this situation, the potential that dropped across the VTS is lowered and becomes substantially lower than the voltage applied to the structure, i.e., the VTS loses the properties of a system that optimizes the distribution of the potential.

The practical conclusion from this study lies n the statement that, in silicon detectors of nuclear radiation, which operate at high radiation loads and high voltages, the observed stability of their characteristics (the lack of breakdown) is governed by the effect of current limited by the space charge, i.e., by suppression of the electric field in regions where the subthreshold high electric field gives rise to the injection of charge carriers from the contact to the detector bulk. The aforementioned conclusion confirms this mechanism, which was suggested previously by Eremin et al. [7].

ACKNOWLEDGMENTS

This study was supported by a grant of the scientific school of the President of the Russian Federation (grant no. NSh-3306.2010.2), by the program "Experimental and Theoretical Studies of Basic Interactions Related to Experiments at the Accelerator Complex CERN", and in the context of the scientific program of collaboration CERN-RD-50.

REFERENCES

1. E. M. Verbitskaya, V. K. Eremin, N. N. Safonova, I. V. Eremin, Yu. V. Tubol'tsev, S. A. Golubkov, and K. A. Kon'kov, Semiconductors **45**, 536 (2011).
2. Z. Le, E. Verbitskaya, V. Eremin, B. Dezillie, W. Chen, and M. Bruzzi, Nucl. Instrum. Methods Phys. Res. A **476**, 628 (2002).
3. H. W. Kraner, Z. Li, and E. Fretwurst, Nucl. Instrum. Methods Phys. Res. A **326**, 350 (1993).
4. V. Eremin, N. Strokan, E. Verbitskaya, and Z. Li, Nucl. Instrum. Methods Phys. Res. A **372**, 388 (1996).
5. S. M. Sze, *Physics of Semiconductors Devices* (Wiley Intersci., New York, 1981; Mir, Moscow, 1984), Vol. 1.
6. V. Eremin, E. Verbitskaya, and Z. Li, Nucl. Instrum. Methods Phys. Res. A **476**, 537 (2002).
7. V. Eremin, E. Verbitskaya, A. Zabrodskii, Z. Li, and J. Härkönen, Nucl. Instrum. Methods Phys. Res. A **658**, 145 (2011).

Translated by A. Spitsyn